Sudden Productivity Collapse Associated with the Triassic-Jurassic Boundary Mass Extinction

P. D. Ward, *et al.*

Science **292**, 1148 (2001);
DOI: 10.1126/science.1058574

in some studies to spatial moment distributions on faults simply by adjusting them by a constant rupture velocity. This procedure makes the widespread implicit assumption that spatial complexity always manifests itself as complexity in the moment rate function, and complexity of plate boundaries in the past have been judged by looking at time functions of the source process of individual earthquakes. For this earthquake, such an assumption would have precluded identification of the eastward rupture and overestimated the length of the N-S one.

The occurrence of this large- and high-stress drop earthquake shows that large stresses can accumulate in an intraplate region of distributed deformation. The fact that there are no large earthquakes to the east of the IFZ suggests that the region of present-day active seismic deformation is smaller than the region of distributed deformation (Fig. 1) accumulated over millions of years and identified from the long-wavelength gravity field (*2*), a property also seen at the western side of the region. The region of deformation thus appears to be localizing with time onto a narrower N-S region.

References and Notes

1. C. DeMets, R. G. Gordon, D. F. Argus, S. Stein, *Geophys. J. Int.* **101**, 425 (1990).
2. J.-Y. Royer, R. G. Gordon, *Science* **277**, 1268 (1997).
3. R. G. Gordon, *Annu. Rev. Earth Planet. Sci.* **26**, 615 (1998).
4. R. D. Müller, W. R. Roest, J. Y. Royer, L. M. Gahagan, J. G. Sclater, *J. Geophys. Res.* **102**, 3211 (1997).
5. C. Deplus *et al.*, *Geology* **26**, 131 (1998).
6. Supplemental Web material is available at www.sciencemag.org/cgi/content/full/292/5519/1145/DC1.
7. The *P* waves for the largest aftershock are complex, in part because of water reverberations. *P* waves are sensitive to bathymetry, which varies in the source region because of the presence of seamounts and ridges. Hence, detailed modeling of the main shock *P* waves cannot be carried out reliably, although some properties of the rupture, such as directivity, are deduced by inspection of these waves. The *SH* waves, on the other hand, are unaffected by the water reverberations and have simpler waveforms, and hence we are able to reliably model these. The crustal structure CRUST 5.1 for this region (*13*) is consistent with the aftershock *SH* waves, and we used it in this study. We inverted *SH* waves to obtain the fault slip rate history and distribution [see section 3 of Web material (*6*)]. The spatial extent and duration of the parameterized source are taken to be larger than would be expected on the basis of an initial inspection of the aftershock zone and the preliminary moment rate function. This means that the true spatial extent and duration are determined as part of the solution, along with all other source parameters, such as rupture speed and average slip (as listed in Table 1), and not assigned a priori. For this earthquake, we used a 300-km N-S fault centered on the epicenter and a 200-km E-W fault centered on the N-S fault. We divided these faults into 10-km cells along strike. Along the dip direction, we have one cell extending throughout the crust (7 km thick) and a second cell below the crust extending to a depth of 15 km. We used 3-s time steps, and every cell is allowed to slip at every time step, except when this would be in advance of a 6 km s^{-1} wavefront emitted from the hypocenter. We imposed the physically motivated constraint that the moment rate must be positive in all cells at all time steps, which is known to be essential to obtain a stable solution (*14*).
8. We first carried out inversions to obtain the best single rupture plane. We tried many possible faults [see section 4 of Web material (*6*)] close to each of the N-S and E-W nodal planes. No prior assumptions about directivity were made for these inversions. In each of ~75 such inversions, we failed to fit all of the seismograms. In order to fit the stations to the north and east, rupture must have occurred on both nodal planes. Thus, in a series of ~20 further inversions, rupture is simultaneously permitted on both nodal planes, still without any prior assumptions about directivity. The best fitting E-W plane is slightly different from the conjugate plane of the N-S rupture plane, with the exact conjugate plane fitting the data less well. Sixteen further inversions were carried out to investigate the range of moments on each fault plane and the possible locations of the E-W rupture consistent with the data. We found that placing the E-W fault plane south of the epicenter provides a slightly better fit to the data than placing it to pass through the epicenter. Because the E-W rupture initiated while motion was still continuing on the N-S rupture plane and because it has a smaller M_w, its parameters cannot be as well resolved as those for the N-S rupture, and hence we cannot provide their error bars in Table 1. The principal features of the preferred solution that we discuss and interpret are also present in all of our other inversions and can thus be regarded as robust [see section 4 of Web material (*6*)]. To test if any moment could have been released immediately east of the main N-S fault, we searched for the solution with maximum moment released in this region. We found for this case that the total moment on the E-W fault is reduced and does not exceed 40% of its previous value, with all the moment being shifted into this region. However, the resulting deterioration of the fit of the stations to the east indicates that this solution does not possess sufficient directivity to the east, and hence we reject the possibility that substantial moment could have occurred on the E-W fault immediately to the east of the N-S fault.
9. C. Henry, S. Das, J. H. Woodhouse, *J. Geophys. Res.* **105**, 16097 (2000).
10. S. Das, *Geophys. J. Int.* **115**, 778 (1993).
11. G. Pegler, S. Das, *Tectonophysics* **257**, 111 (1996).
12. W. H. F. Smith, D. T. Sandwell, *Science* **277**, 1956 (1997).
13. W. D. Mooney, G. Laske, T. G. Masters, *J. Geophys. Res.* **103**, 727 (1998).
14. S. Das, B. V. Kostrov, *J. Geophys. Res.* **95**, 6899 (1990); S. Das, B. V. Kostrov, *Phys. Earth Planet. Inter.* **85**, 293 (1994).
15. A. M. Dziewonski *et al.*, *Phys. Earth Planet. Inter.* **33–121** (1983–2000).
16. B. Gutenberg, C. F. Richter, *Seismicity of the Earth and Associated Phenomena* (Princeton Univ. Press, Princeton, NJ, 1954).
17. K. Aki, P. G. Richards, *Quantitative Seismology: Theory and Methods* (Freeman, New York, 1980).
18. A. M. Dziewonski, J. H. Woodhouse, in *Proceedings of the International School of Physics "Enrico Fermi," LXXXV, Varenna, 29 June to 9 July, 1982, Italian Physical Society*, H. Kanamori, E. Boschi, Eds. (North-Holland, Amsterdam, 1983), pp. 45–137; *J. Geophys. Res.* **88**, 3247 (1983).

19. D.P.R. is supported by the Salford (U.K.) Local Education Authority and the Oppenheimer Fund of Worcester College, Oxford; C.H. is supported by U.K. Natural Environment Research Council (NERC) studentship GT04/97/ES/217 and a Schlumberger Cooperative Awards in Sciences of the Environment grant. Computations were carried out under NERC grant GR9/03960, and the Oxford seismological data facility was supported by NERC grant GR11534.

29 January 2001; accepted 23 March 2001

Sudden Productivity Collapse Associated with the Triassic-Jurassic Boundary Mass Extinction

P. D. Ward,[1]* J. W. Haggart,[2] E. S. Carter,[3] D. Wilbur,[4] H. W. Tipper,[2] T. Evans[1]

The end-Triassic mass extinction is one of the five most catastrophic in Phanerozoic Earth history. Here we report carbon isotope evidence of a pronounced productivity collapse at the boundary, coincident with a sudden extinction among marine plankton, from stratigraphic sections on the Queen Charlotte Islands, British Columbia, Canada. This signal is similar to (though smaller than) the carbon isotope excursions associated with the Permian-Triassic and Cretaceous-Tertiary events.

The Triassic-Jurassic (T-J) boundary mass extinction, one of the five most severe in Phanerozoic history, led to the demise of as many as 80% of all living species (*1–3*). Unanswered questions about the extinction concern its duration, its severity, and whether it affected global productivity. The extinction in marine strata has recently been dated at 199.6 ± 0.3 million years ago (Ma) by means of high-resolution U-Pb zircon geochronometry (*4*), but it is unknown whether the extinctions were synchronous on land and in the sea, because this date seems slightly later than the extinction dated on land (*5*). It has been suggested that the T-J extinction, unlike the Permian-Triassic (P-T) and Cretaceous-Tertiary (K-T) events, did not affect the carbon cycle long enough to cause a clear perturbation in δ^{13} organic carbon ($\delta^{13}C_{org}$) (*6*),

[1]Department of Earth and Space Sciences, University of Washington, Seattle, WA 98195, USA. [2]Geological Survey of Canada, Vancouver, British Columbia V6B 5J3, Canada. [3]Department of Geology, Portland State University, Portland, OR 97207, USA. [4]Department of Oceanography, University of Washington, Seattle, WA 98195, USA.

*To whom correspondence should be addressed.

leading to the conclusion that this mass extinction did not significantly affect bioproductivity on a global basis or the long-term burial of organic carbon. We present here a record of a rapid and negative excursion in carbon isotopes at the top of the uppermost stage of the Triassic and including the T-J boundary, from a stratigraphic section that appears relatively unaffected by diagenesis. This isotopic anomaly is coincident with a sudden extinction of marine plankton (Radiolaria) at the paleontologically defined T-J boundary.

We studied the uppermost Peril (Triassic: Upper Norian) and Sandilands (Triassic-Jurassic: Rhaetian to Pliensbachian) formations at two sites on the Queen Charlotte Islands, British Columbia, Canada: Kennecott Point (Fig. 1) (latitude 53°54′48.4″N, longitude 133°09′17.8″W) and Kunga Island [a proposed candidate for the type section of the T-J boundary (*7*)] (latitude 52°45′31.4″N, longitude 131°33′36.6″W), located approximately 165 km southeast of Kennecott Point. The uppermost Peril Formation consists of black calcareous shale and siltstone, whereas the overlying Sandilands Formation consists of laminated, thinly bedded, organic-rich siltstone and black shale interbedded with thicker turbiditic sandstone and tuff (*8*). At both sections, the T-J boundary is placed, on biostratigraphic grounds, at the base of the Lower Hettangian *Canopum merum* radiolarian zone, which is equivalent to the North American *Psiloceras* assemblage of the ammonoid standard zonal sequence (*9*). Stratigraphic sections at both localities have been correlated paleontologically (*10*), and the boundary at Kunga Island (Fig. 2) lies 6.3 m above a tuff dated to 199.6 Ma (*4*).

Bulk samples of black shale were collected stratigraphically from both sections and analyzed for organic carbon with mass spectroscopy (*11*). Total organic carbon (TOC) at both sections varies from 1 to 6% for the samples. At Kennecott Point (Fig. 1), there is no significant correlation between TOC and $\delta^{13}C_{org}$ (R^2 = 0.006). At Kunga Island, however, there is a significant correlation (R^2 = 0.64), which suggests that extensive diagenetic alteration of these strata may have occurred.

At both Kennecott Point and Kunga Island, a significant turnover of radiolarian fossils occurs at the level of the paleontologically defined T-J boundary. In neither section is there any discernible lithological change across this interval. At Kunga Island, more than 60 species of radiolarians disappear across the boundary interval (*12*), whereas more than 50 species disappear in the Kennecott Point section (*13*). The disappearance of the Kennecott Point radiolarians is less precisely located, because there is a lack of radiolarian-bearing concretions over a 6-m-thick stratigraphic interval in which the extinction level must lie. The highest Rhaetian (Triassic) ammonoid recovered at Kennecott Point, *Choristoceras rhaeticum*, was found 16 m below the boundary, and the lowest Hettangian ammonite, *Psiloceras pacificum*, was found 6 m above the boundary. No ammonites

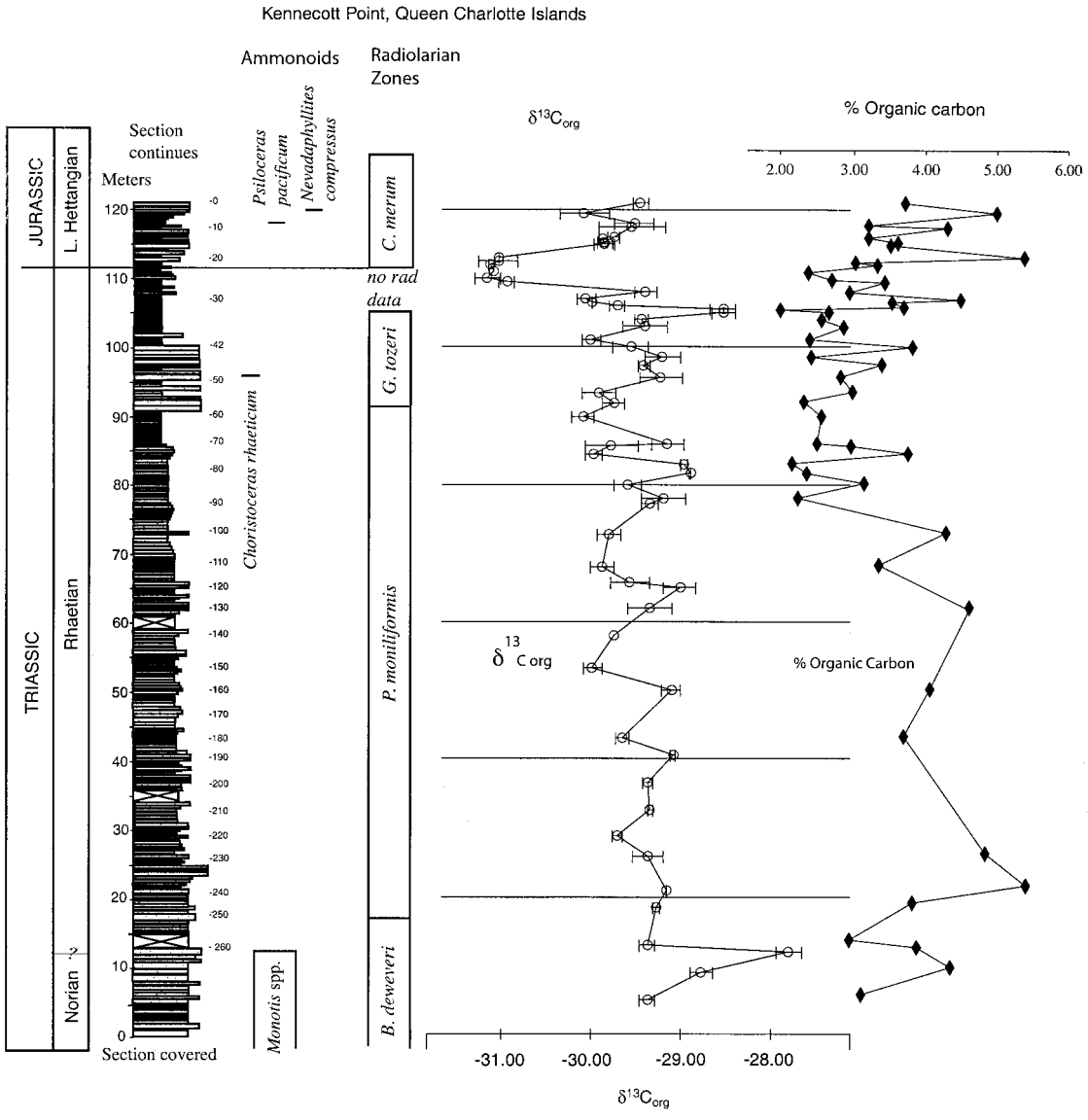

Fig. 1. Measured stratigraphic section from Kennecott Point, showing fossil ranges and results from isotopic analysis of bulk samples. Both $\delta^{13}C_{org}$ and TOC are separately plotted. For $\delta^{13}C_{org}$, each point represents the mean of a duplicate run; error bars were computed based on the variance and reproducibility of sample and standards on a particular run. The T-J boundary is based on first occurrences of elements of the *C. merum* radiolarian zone.

have been recovered near the boundary interval at Kunga Island.

Bulk samples collected across the boundary interval at Kennecott Point yielded a stratigraphically restricted (<5 m), ~2 per mil (‰) change in $\delta^{13}C_{org}$, followed by a return to values that were slightly more negative than those beneath this excursion. Although the magnitude of the excursion is not as great as that seen at most P-T or K-T boundary sites, what stands out about the isotope record that we have recovered from the Kennecott Point boundary interval is that the absolute values are well below the background variation in the rest of the section (which spans all of the Rhaetian Stage and the upper part of the Norian and lower part of the Hettangian stages) and are defined by multiple samples.

Samples collected from the Kunga Island section also show a significant deviation from background $\delta^{13}C_{org}$ values across the T-J boundary. Unlike the Kennecott Point results, however, the deviation in $\delta^{13}C_{org}$ is positive rather than negative and is defined by a single sample. In its positive trend, the Kunga Island excursion thus resembles the isotopic record from the T-J section at Kendelbach, Austria, which has been ascribed to diagenesis (*6*). Although the positive correlation of percent TOC and $\delta^{13}C_{org}$ at Kunga Island suggests that the observed isotopic values obtained from there may have been compromised by diagenesis, the Kennecott Point samples show no such evidence either from isotopes or lithology (*14*).

Although the sudden extinction of radiolarians at the T-J boundary is the most important bioevent in our two studied sections, there is also a second event recorded lower in the Kennecott Point section, at the Norian/Rhaetian boundary, that is most prominently marked by the disappearance of monotid bivalves. The extinction of monotid bivalves in the section is associated with a gradual change in lithology, from massive and bioturbated black calcareous mudstone and siltstone with abundant bedding-plane concentrations of *Monotis* spp. in bituminous facies of the Peril Formation to thinly laminated black shale interbedded with more massive turbiditic siltstone and fine sandstone composing the Sandilands Formation. This lithological change extends over a few tens of meters. Ammonoid abundance also decreases significantly at this level, and their preservation changes from entire (but flattened) body fossils to impressions of shells with siphuncular structures preserved in three dimensions within the phragmocone outline. Trace fossil assemblages also change here, with an increase in *Chondrites* on bedding planes in the dark shale facies, suggesting increasingly anaerobic bottom conditions (*8*). As shown in Fig. 1, this extinction interval is marked by an increase in $\delta^{13}C_{org}$ values in two samples, coincident with the disappearance of monotids. Further sampling is needed to ascertain whether this isotopic change is significant and correlated with the extinction event.

The pattern of sudden extinction coincident with a $\delta^{13}C_{org}$ decrease at the Rhaetian/Hettangian (T-J) boundary at Kennecott Point is compatible with a sudden biological crisis affecting marine productivity. As yet there is no reliable means of dating the duration of this event in the Queen Charlotte Islands sections (although the presence of ashes will make such analyses feasible in the future). As a rough estimate, however, if the Rhaetian Stage duration is taken as 6 million years in length (*3*), and assuming constant sedimentation rate at Kennecott Point during that time, then the duration of the isotopic excursion at the Kennecott Point section would be about 500,000 years in length, whereas the extinction event itself was likely on the order of 50,000 years or even less.

Other possibilities that could explain the observed pattern in carbon isotopes include a decrease in organic carbon burial coincident with the biodiversity decline of Radiolaria, and/or a rapid recycling of isotopically light bottom water caused by a shallowing of the water column pycnocline. However, it seems a more parsimonious interpretation that a single short-term event caused the observed isotopic pattern at the Kennecott Point T-J boundary. This pattern exhibits similarity with those seen at extinction boundaries such as the K-T and P-T, where extraterrestrial impact scenarios have been invoked.

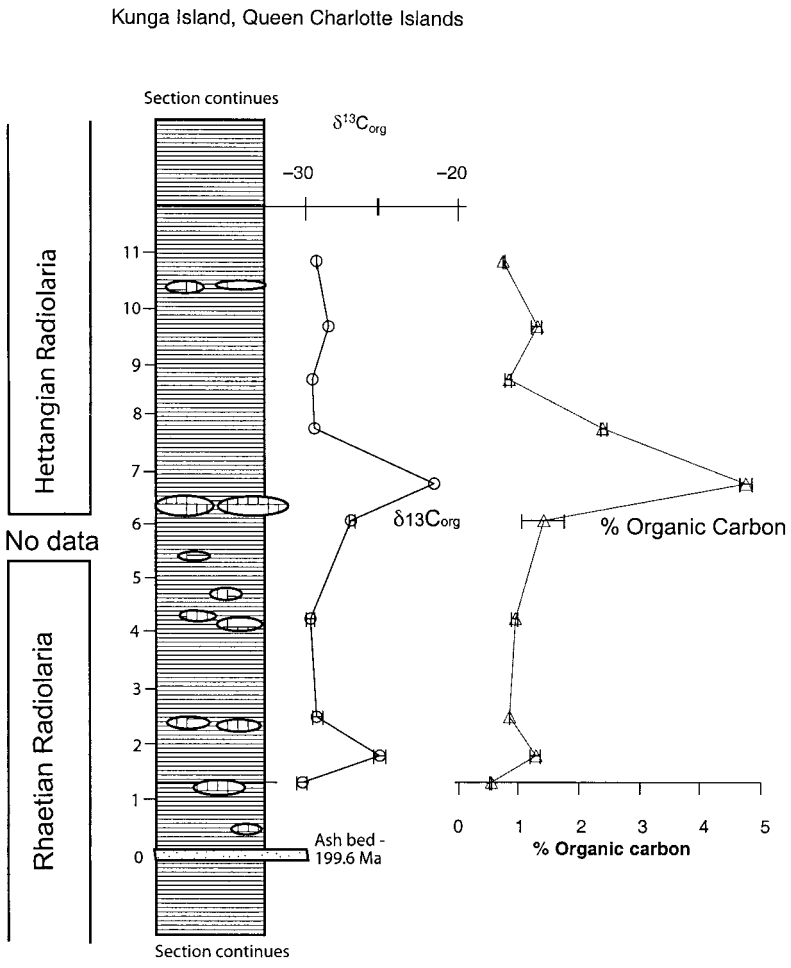

Fig. 2. Measured stratigraphic section of the T-J boundary interval at Kunga Island, showing positive correlation of percent TOC and $\delta^{13}C_{org}$, suggesting diagenesis. The section is composed of massive thinly bedded siltstone. Data are presented as in Fig. 1.

References and Notes

1. N. D. Newell, *Geol. Soc. Am. Spec. Pap.* **89**, 63 (1967); A. Hallam, *Geol. Soc. London Spec. Pap.* **102**, 231 (1996).
2. J. J Sepkoski, *Paleobiology* **19**, 43 (1993).
3. A. Hallam, P. Wignall, *Mass Extinctions and Their Aftermath* (Oxford Univ. Press, Oxford, 1997).
4. J. Pálfy *et al.*, *Geology* **28**, 39 (2000).
5. G. R. Dunning, J. P. Hoydch, *Geology* **18**, 795 (1990).
6. R. Morante, A. Hallam, *Geology* **24**, 391 (1996).
7. E. S. Carter, H. W. Tipper, *Int. Subcomm. Jurassic Stratigr. Newsl.* 27 (1999).
8. A. Desrochers, M. J. Orchard, *Geol. Surv. Can. Pap.* **90-10**, 163 (1991).
9. H. W. Tipper, J. Guex, *Geobios Mem. Spec.* **17**, 477 (1994).
10. E. S. Carter, P. A. Whalen, J. Guex, *Geol. Surv. Can. Bull.* **496**, 27 (1998).

11. Isotopic analyses were performed in the University of Washington laboratory of P. Quay. Isotope analyses were done with two methods, both ultimately calibrated versus National Bureau of Standards–19 (NBS-19), for ^{13}C = 1.95‰ versus the Vienna

PeeDee Belemnite (VPDB) standard and for ^{15}N = 0.0‰ versus air nitrogen. The first anaylsis (sealed-tube combustion with subsequent measurement on a Finnigan MAT 251 mass spectrometer) has a reproducibility of ± 0.08‰ for organic standards. The second analysis [elemental analyzer–continuous-flow isotope ratio mass spectrometry (EA/CFIRMS)] used a Carlo Erba NC2500 interfaced through a Finnigan CONFLO II to a Finnigan Delta XL mass spectrometer. Reproducibility in this system averages ±0.12‰ for organic standards and homogenous natural samples. The EA/CFIRMS analyses were calibrated as follows: For each sample, $\delta^{15}N$ and $\delta^{13}C$ were measured versus a pulse of 99.999% pure standard gas injected into the mass spectrometer source immediately before or after the sample pulse eluted from the EA. Because the isotope ratios obtained were dependent on mixing ratios of carrier gas and dilutant in the CONFLO, the ratios were normalized to a known organic standard run with the samples under the same conditions. To verify that the corrections were normalized properly, each run also contained four aliquots of a natural sample whose ratios were known from sealed-tube combustion. This natural sample had a precision identical to the organic standard (±0.12‰) and the average of four determinations was within a range of ±0.1‰ of its correct value. Each autosampler run contained seven organic acid standards, four natural sample standards, and 40 samples and blanks. Blanks typically were less than 1% of the sample amount. Samples were prepared for analysis by grinding, followed by weighing into silver boats (measuring 5 mm by 9 mm) and acidification with 20 μl of 50% HCl. After air drying overnight at 50°C, the sample boats were sealed and measured as follows: Isotope analyses were performed by EA/CFIRMS, using a Carlo Erba NC2500 interfaced through a Finnigan CONFLO II to a Finnigan Delta XL mass spectrometer. Sample isotope ratios were normalized in each run to the values obtained for an organic standard with known isotope ratios calibrated in sealed-tube combustions versus NBS-19 for $\delta^{13}C$ = 1.95‰ versus VPDB and for $\delta^{15}N$ = 0.0‰ versus air nitrogen. Precision in this system averages ±0.12‰ for organic standards and homogenous natural samples. Accuracy, as measured by including repeats of a natural sample of known isotopic ratio in each run, was ±0.10‰. All isotope ratios are expressed in delta notation, or parts per thousand deviation from VPDB, where $\delta^{13}C = \{[(^{13}C/^{12}C)_{sample}/(^{13}C/^{12}C)_{VPDB}] - 1\} \times 1000$.

12. E. S. Carter, *Mem. Geol.* (*Lausanne*) **11**, 175 (1993).
13. E. S. Carter, unpublished results of 2000 sampling at Kennecott Point.
14. M. J. Orchard, P. J. L. Forster, *Geol. Surv. Can. Pap.* **90-10**, 453 (1991).
15. Supported by a grant from NSF (H. Lane, program administrator) to P.D.W. and by Geological Survey of Canada Project number 870070.

22 December 2000; accepted 28 March 2001

African Origin of Modern Humans in East Asia: A Tale of 12,000 Y Chromosomes

Yuehai Ke,[1]* Bing Su,[2,1,3]* Xiufeng Song,[1] Daru Lu,[1] Lifeng Chen,[1] Hongyu Li,[1] Chunjian Qi,[1] Sangkot Marzuki,[4] Ranjan Deka,[5] Peter Underhill,[6] Chunjie Xiao,[7] Mark Shriver,[8] Jeff Lell,[9] Douglas Wallace,[9] R Spencer Wells,[10] Mark Seielstad,[11] Peter Oefner,[6] Dingliang Zhu,[12] Jianzhong Jin,[1] Wei Huang,[12,13] Ranajit Chakraborty,[3] Zhu Chen,[12,13] Li Jin[1,3,13] †

To test the hypotheses of modern human origin in East Asia, we sampled 12,127 male individuals from 163 populations and typed for three Y chromosome biallelic markers (YAP, M89, and M130). All the individuals carried a mutation at one of the three sites. These three mutations (YAP+, M89T, and M130T) coalesce to another mutation (M168T), which originated in Africa about 35,000 to 89,000 years ago. Therefore, the data do not support even a minimal in situ hominid contribution in the origin of anatomically modern humans in East Asia.

The "Out-of-Africa" hypothesis suggests that anatomically modern humans originated in Africa about 100,000 years ago and then spread outward and completely replaced local archaic populations outside Africa (*1*, *2*). This proposition has been supported by genetic evidence and archaeological findings (*3*–*9*). The replacement in Europe was supported by recent ancient DNA analyses, which ruled out the contribution of Neanderthals to modern Europeans (*10*, *11*). However, it has been argued that the abundant hominid fossils found in China and other regions in East Asia (e.g., Peking man and Java man) demonstrate continuity, not only in morphological characters but also in spatial and temporal distributions (*12*–*16*). In this report, we test the competing hypotheses of modern Asian human origins using Y chromosome polymorphisms.

We sampled 12,127 male individuals from 163 populations across Southeast Asia, Oceania, East Asia, Siberia, and Central Asia and typed for three Y chromosome biallelic markers (YAP, M89, and M130) (*17*, *18*) (Table 1). Being a single-locus multiple-site (i.e., haplotype) system, the Y chromosome is one of the most powerful molecular tools for tracing human evolutionary history (*5*, *9*, *19*–*21*). In previous Y chromosome studies, an extreme geographic structure was revealed in global populations in which the oldest clade represents Africans and the younger ones represent some Africans and all non-African populations (*21*). One Y chromosome polymorphism (C to T mutation) at the M168 locus is shared by all non-African populations and was originally derived from Africa on the basis of a study of 1062 globally representative male individuals (*21*). The age of M168 was estimated at 44,000 years (95% confidence interval: 35,000 to 89,000 years), marking the recent Out-of-Africa migrations (*21*). Under the M168T lineage, there are three major derived sublineages defined by polymorphisms at loci YAP (Alu insertion) (*5*), M89 (C to T mutation), and M130 (C to T mutation, also called RPS4Y) (Fig. 1) (*21*, *22*). Therefore, these three markers can be used to test the completeness of the replacement of modern humans of African origin in East Asia. An observation of a male individual not carrying one of the three polymorphisms would be indicative of a potential ancient origin and could possibly lead to the rejection of such completeness.

Each of the 12,127 samples typed carried one of the three polymorphisms (YAP+, M89T, or M130T) (Table 1). In other words, they all fall into the lineage of M168T that was originally derived from Africa. Hence, no ancient non-African Y chromosome was found in the extant East Asian populations ($P = 5.4 \times 10^{-6}$ assuming a frequency of 1/1000 of local contribution in the extant populations), suggesting an absence of either an independent origin or a 1,000,000-year shared global evolution. This result indicates that modern humans of African origin completely replaced earlier populations in East Asia.

[1]State Key Laboratory of Genetic Engineering, Institute of Genetics, School of Life Sciences, Fudan University, 220 Handan Road, Shanghai, China 200443, and Morgan-Tan International Center for Life Sciences, Shanghai, China. [2]Kunming Institute of Zoology, the Chinese Academy of Sciences, Kunming, China. [3]Human Genetics Center, University of Texas–Houston, 1200 Herman Pressler E547, Houston, TX 77030, USA. [4]Eijkman Institute for Molecular Biology, Jakarta, Indonesia. [5]Department of Environmental Health, University of Cincinnati, Cincinnati, OH 45267, USA. [6]Department of Genetics, Stanford University, Stanford, CA 94305, USA. [7]Department of Biology, Yunnan University, Kunming, China. [8]Department of Anthropology, Pennsylvania State University, University Park, PA 16802, USA. [9]Center for Molecular Medicine, Emory University School of Medicine, Atlanta, GA 30322, USA. [10]Wellcome Trust Center for Human Genetics, University of Oxford, UK. [11]Program for Population Genetics, Harvard School of Public Health, Boston, MA 02115, USA. [12]Shanghai Second Medical University, Shanghai, China. [13]National Human Genome Center at Shanghai, China.

*These authors contributed equally to this work.
†To whom correspondence should be addressed. E-mail: ljin@fudan.edu or ljin@sph.uth.tmc.edu